Electronic Supplementary Material (ESI) for Nanoscale.
This journal is © The Royal Society of Chemistry 2014

Supplementary information for Quantum-confined single photon emission at room temperature from SiC tetrapods

Stefania Castelletto[a], Zoltán Bodrog[b], Andrew P. Magyar[c], Angus Gentle[d] Adam Gali[b,e], and Igor Aharonovich[d]

[a] School of Aerospace, Mechanical and Manufacturing Engineering RMIT University, Melbourne, Victoria 3000, Australia;

[b] Institute for Solid State Physics and Optics, Wigner Research Centre for Physics, Hungarian Academy of Sciences, P.O.B. 49, H-1525, Budapest, Hungary;

[c] Center for Nanoscale Systems, Harvard University, Cambridge MA 02138 USA;

[d] School of Physics and Advanced Materials, University of Technology Sydney, Ultimo, NSW 2007, Australia;

[e] Department of Atomic Physics, Budapest University of Technology and Economics, Budafokiút 8. H-1111, Budapest, Hungary

[*]Correspondence should be addressed to Igor Aharonovich
igor.aharonovich@uts.edu.au

Model and simulations

In our simplified model, the tetrapod system may be described as 4H (leg)-3C (core)-4H (leg) quasi one-dimensional structure. In the other two dimensions we assume that the usual Bloch-states of the perfect 4H and 3C crystals are the solution. Upon illumination the excited electrons and holes fast relax to the conduction band edge and valence band edge, respectively, where the 4H (leg)-3C (core)-4H (leg) "superlattice" creates quantum confinement for these electron and hole along the length of 4H legs. The bound exciton states may appear in the quantum confined region, for which the following one-dimensional Hamiltonian (in atomic units) has to be solved,

$$H = -\frac{\Delta_e}{2m_e^*} - \frac{\Delta_e}{2m_e^*} + V_{CBM} + V_{VBM} - \frac{1}{\varepsilon}\frac{1}{|r_e - r_h|}$$

where m_e* and m_h* are the effective masses of electrons and holes, respectively, and r_e and r_h are their positions. The potentials acting on them (V_{CBM} and V_{VBM}) depend on tetrapod properties (ΔV, d_{3C}, r_{leg1}, r_{leg2}) parametrically. Here, ΔV parameter refers to the steepness of the potential (see Figure 2a) which is associated with the asymmetry in the geometry of 4H(legs) in the tetrapod. The zero levels of V_{CBM} and V_{VBM} are set to their respective levels at the end of legs. ε is the relative dielectric constant of silicon carbide. The materials parameters are taken from bulk crystal. We numerically solved this equation at different ΔV and d_{3C}

parameters. The calculated lowest energy corresponds to the energy of the exciton which emits light after radiative recombination. The higher energy excited states are also bound to the potential, so the exciton remains stable at elevated temperatures.

The length of 4H SiC leg is about 100 nm so the band structure of bulk 4H SiC is not modified along the axis of the leg. The diameter of ~50 nm may cause dielectric confinement along the axes perpendicular to the axis of the leg. However, the dielectric confinement may alter by few meV the band structure of bulk 4H SiC, an effect that can be neglected. Thus, bulk parameters of 4H and 3C SiC polytypes are used to set-up the models such as band gaps and band alignment between 3C and 4H SiC polytypes, dielectric constants and the effective masses of electron and holes.

On the 3C-4H boundary, the difference of conduction band minima (CBM) is 0.92eV (4H is higher), and the difference of valence band maxima (VBM) is 0.05eV (4H is higher again). As a simple but acceptable approximation, we set the effective mass of electrons in both parts to 0.33 in atomic units, while the effective mass of holes is generally 1.35 in atomic units [1-2]. For the relative dielectric constant of SiC we use a general approximate value of 9.8[3-4].

To understand the optical properties of the tetrapods, we performed a quantum mechanical simulation of its band structure. The cubic and hexagonal polytypes of SiC have substantially different band gaps that along with the nanoscale geometry of the tetrapod create a quantum well within the complex tetrapod band structure. Between hexagonal and cubic layers of 4H-SiC, there is a charge asymmetry of about 0.02e according to the Mulliken analysis of hexagonal and cubic Si sites[5-6]. Therefore, the fact that a leg ends with one type of layer or another can make difference in the electric field (due to spontaneous polarization) present in the legs where the potential difference is depicted as eV in Fig. 2A. Subsequently, a triangular quantum well is formed leading to spatially indirect exciton transitions between electrons in the 3C region to holes in the 4H-SiC.

These parameters are used to set-up the kinetic energy and potential energy of the quasi one-dimensional Hamiltonians. The single-particle equation of the Hamiltonian can be solved separately for the electron (conduction band edge) and for the hole (valence band edge) by numerical integration of the Hamiltonians. These two potential curves are separated by the band gap. The electron and hole form an exciton where the electron and hole is attracted by Coulomb-interaction. According to previous studies, the exchange interaction is much smaller than direct Coulomb-interaction[7-8], thus we neglect the exchange interaction.

The total exciton energy, is given by $E_{exc} = E_e + E_h + E_C$ where E_e, E_h is the one-particle ground-state eigenenergy of electron and the hole, respectively. E_C is the opposite of Coulomb interaction energy in order to compensate double counting. We note that we introduce E_C to

the system in a self-consistent manner, so that the electron and hole wave functions as well as their corresponding single particle E_e, E_h eigen-energies are modified. The Coulombic binding energy of the exciton may be defined as an energy difference of $E_e + E_h$ before taking into account the interaction between the electron and hole and E_{exc} defined above.

As a result, the total exciton energy in the symmetric and nearly symmetric systems is around 2 eV, which corresponds to 600-610 nm wavelength for an emitted photon if the photon energy is $E_{\text{gap}} - E_{exc}$, where E_{gap} is the band gap of 4H-SiC (where we set the zero level of electron and hole energy as the conduction band minimum and valence band maximum, respectively). This result approximately reproduces the position of the bluest peaks in tetrapod photoluminescence spectra. In cases where the hole and electron do not overlap, the total energy of exciton can be adjusted by the slope of the potential well. This gives deeper energy minima for the two constituents of exciton, resulting in smaller energy that can be won for the emitted photon. An asymmetry of ~ 1.0 eV gives the longest wavelengths that were measured (around 800 nm). Finally, the anisotropy of photoluminescence signal can be explained by the fact that the direction defined by the maximum and minimum potential values on the core boundary break the original symmetry of tetrapods through aligning the electron and hole along it. Figure S1 depicts the positions of the hole and electron along the tetrapod. Note that 10 nm core size was selected for the purpose of illustration, as an upper limit. It is likely that every tetrapod will have a slightly different core size.

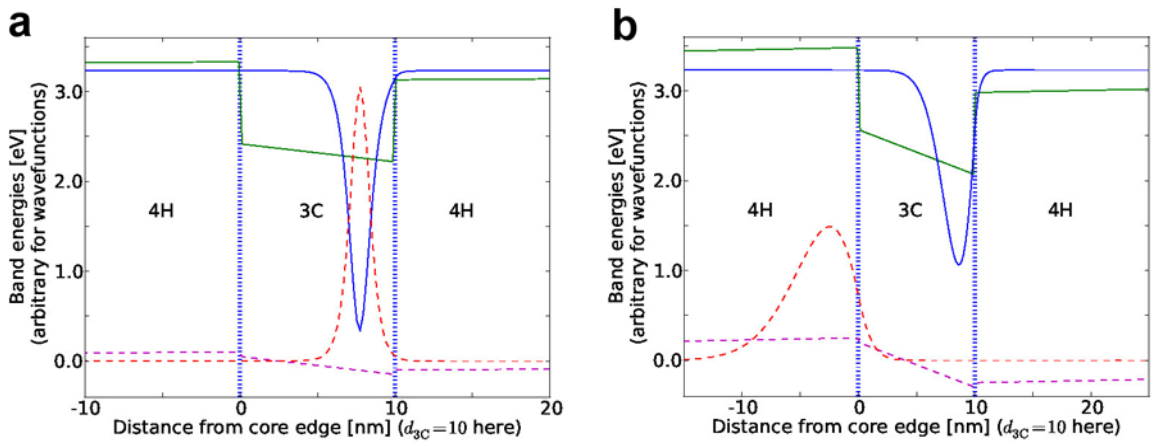

Figure S1 (a). Positions of the hole and electron in situations with relatively low gradient of the potential. Potentials and wavefunctions are shown, electronic graphs are solid lines, those of the hole are dashed. The binding energy of exciton is the Coulomb energy, which makes exciton energies in such totally overlapping situations almost independent of any external parameter. (b) Positions of hole and electron when the potential is steep in the core region.

Reachable potential differences are greater than Coulomb attraction, which makes the possible lowest exciton energy lower than in figure 1c, making the energy yield of exciton annihilation lower, and the emitted photon red shifted).

Additional optical measurements

Figure S2(a) shows the distribution of the central emission wavelength for individual tetrapods in the near infrared spectral range at room temperature. Figure S2(b) shows a saturation curve recorded from a single tetrapod at room temperature. The black squares are the experimental data and the red curve is the theoretical fit.

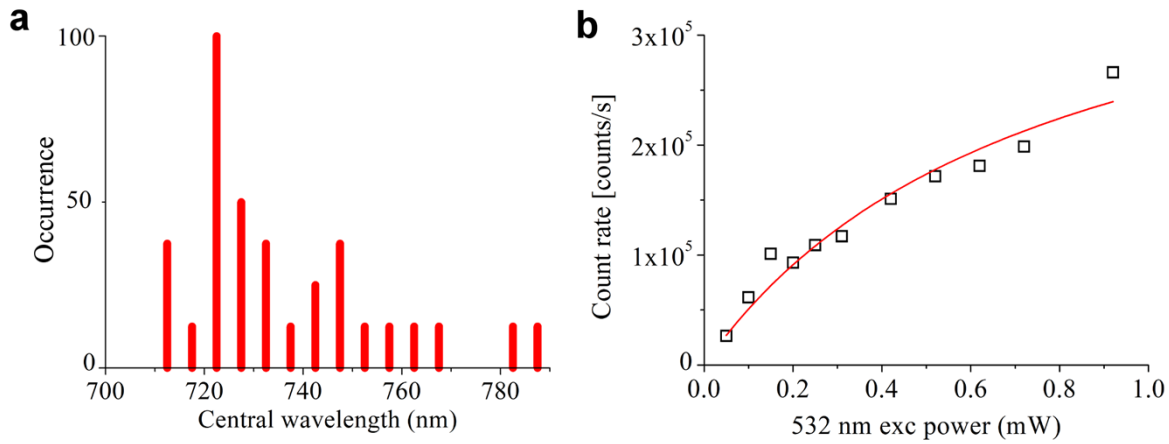

Figure S2. (a) Central emission wavelength for individual tetrapods. (b) Saturation curve of a single tetrapod. The measurements in (a) and (b) were recorded at room temperature.

Structural characterization

Figure S3 shows a representative HRTEM image of a single tetrapod. Asymmetry between the legs is evident. The dark region in the center is a superposition of the core and the fourth leg, which is oriented perpendicular to the plane of the image. Inset is a zoom over the interface between the core and the leg, showing the SiC lattice fringes.

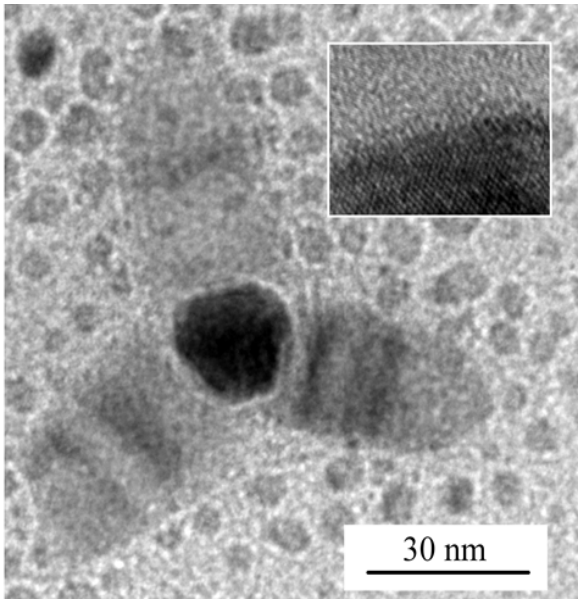

Figure S3. A representative HRTEM image of a single tetrapod. Inset is a zoom over the interface between the core and the leg, showing the SiC lattice fringes.

Finally, figure S4 shows an SEM image of the tetrapods, further elucidating the clear anisotropy.

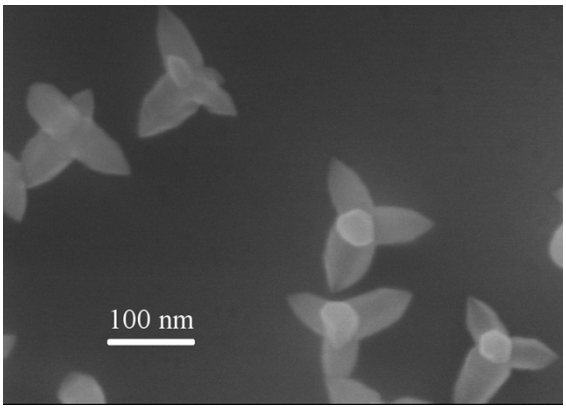

Figure S4. SEM image of the tetrapods.

References

1. Volm, D.; Meyer, B. K.; Hofmann, D. M.; Chen, W. M.; Son, N. T.; Persson, C.; Lindefelt, U.; Kordina, O.; Sörman, E.; Konstantinov, A. O.; Monemar, B.; Janzén, E., *Phys. Rev. B* **1996,** *53* (23), 15409-15412.
2. Persson, C.; Lindefelt, U., *J. Appl. Phys.* **1997,** *82* (11), 5496-5508.
3. Patrick, L.; Choyke, W. J., *Phys. Rev. B* **1970,** *2* (6), 2255-2256.
4. Pernot, J.; Zawadzki, W.; Contreras, S.; Robert, J. L.; Neyret, E.; Di Cioccio, L., *J. Appl. Phys.* **2001,** *90* (4), 1869-1878.
5. Qteish, A.; Heine, V.; Needs, R. J., *Phys. Rev. B* **1992,** *45* (12), 6534-6542.
6. Deák, P.; Buruzs, A.; Gali, A.; Frauenheim, T., *Phys. Rev. Lett.* **2006,** *96* (23), 236803.
7. Royo, M.; Climente, J. I.; Movilla, J. L.; Planelles, J., *Journal of Physics: Condensed Matter* **2011,** *23* (1), 015301.
8. Janssens, K. L.; Partoens, B.; Peeters, F. M., *Phys. Rev. B* **2001,** *64* (15), 155324.